Supporting Information

A Long-Term Stable Zinc Metal Anode Enabled by Mannitol Additive

Dongdong Zhang[1], Jin Cao[2*], Zhiqiang Dai[3], Rungroj Chanajaree[4], Chenwu Yang[4], Xiang Wu[1], Xinyu Zhang[3*], Jiaqian Qin[4,5*]

[1]School of Materials Science and Engineering, Shenyang University of Technology, Shenyang 110870, China

[2]College of Materials and Chemical Engineering, China Three Gorges University, Yichang, Hubei 443002, China

[3]State Key Laboratory of Metastable Materials Science and Technology, Yanshan University, Qinhuangdao 066004, China

[4]Metallurgy and Materials Science Research Institute, Chulalongkorn University, Bangkok 10330, Thailand

[5]Center of Excellence in Responsive Wearable Materials, Chulalongkorn University, Bangkok 10330, Thailand

*Corresponding Author. E-mail: caojin@ctgu.edu.cn (J. C); xyzhang@ysu.edu.cn (X.Z.); jiaqian.q@chula.ac.th (J. Q.)

Experimental section

Preparation of electrolytes

2 mol L^{-1} $ZnSO_4$ electrolyte (ZSO) was obtained by dissolving zinc sulfate heptahydrate (Adamas Reagent Co. Ltd.) in deionized water. The Mannitol (Adamas Reagent Co. Ltd.) was added into $ZnSO_4$ electrolyte and stirred for 1 hours, and then keep in room temperature for 24 hours. The concentration of TA was controlled at 0.02 M.

Characterization

X-ray diffraction (XRD) measurement were performed on a Rigaku D X-ray diffractometer with Cu K radiation. The morphology was conducted by scanning electron microscopy (SEM. Hitachi S4800) and 3D measuring laser microscope (Olympus LEXT OLS5000). Raman spectroscopy was conducted on a Thermo Fisher DXR. Fourier Transform infrared spectroscopy (FTIR) was performed with a Perkin Elmer, Spectrum One 2. Bruker.

Electrochemical performance

The electrochemical performance of the as-prepared electrolytes was investigated by assembling the coin cells (CR2032) with zinc foil anode. And the cathodes were prepared via mixing the commercial α-MnO_2 cathode (Taiyuan Lizhiyuan Technology Co. Ltd.), conductive carbon (Canrd) and PVDF (Canrd) at the mass ratio of 7:2:1, and then coating the slurry on stainless steel. The average mass loading of the active materials was about 2 mg cm^{-2}. After drying under vacuum at 80 °Cs for 12 h, cutting into round electrode pieces with a diameter of 14 mm. The as-prepared electrolytes

(TA+ZSO, ZSO) were served as electrolytes. The galvanostatic charge/discharge (GCD) measurement was performed to identify the rate performance and cycling stability (BTS, CT-4008, Neware, China). The cyclic voltammetry (CV) profiles of the materials were recorded on a CHI 660E workstation (China). The linear polarization curves were performed on a CHI 660E in the potential range from -1.3 to -1.0 V, the Ag/AgCl electrode and platinum foil were severed as reference and counter electrodes, respectively.

Calculation section

The interfacial charge transfer is further investigated by exchange current density (j_0) obtained by using the simplified Butler–Volmer equation [1]:

$$j_0 = \frac{RT}{FAR_{ct}} \quad (1)$$

where R, T, F, and A are the universal gas constant, the temperature, the Faraday constant, and the interfacial area, respectively.

DFT calculations

Density functional theory (DFT) was carried out to obtain the binding interaction energies for MAnnitol-H_2O, Mannitol-Zn^{2+}, and Zn^{2+}-H_2O. The geometry optimization was carried out by using PBE/def2-svp level, and the energy calculations were then calculated by using PBE/def2-tzvp level. The basis set super position error (BSSE) has been considered [2-4]. The ORCA package [5] has been used for all calculations. The binding energies for Mannitol and each adsorbed molecule were calculated using Eq.

(2):

$$\Delta E_B = \Delta E_{cpx} - \Delta E_{Mannitol} - \Delta E_m \quad (2)$$

where ΔE_B is the binding energy (kcal mol^{-1}), ΔE_{cpx} is the complex energy, $\Delta E_{Mannitol}$ is the Mannitol energy, and ΔE_m is the energy of H_2O or Zn^{2+}.

MD simulations

The structural and adsorption properties of complexing agent (Mannitol) systems with the $ZnSO_4$ and water molecules, were investigated by using the classical molecular dynamics (MD) simulations. The DLPOLY 4.09 package [6] was used for this study. The starting box size was 50×50×50 Å^3 and the simulations were performed under the Nose-Hoover ensemble [7, 8] at the temperature of 298 K. The periodic boundary conditions and the minimum image convention were applied. The cutoff radius for short-ranged interaction is 12 Å and the long-ranged interaction was treated by the Ewald summation method [9]. The 10 $ZnSO_4$ and 1000 water molecules were randomly added into each simulation system. To equilibrate the simulation box size, the simulations were first carried out under NPT ensemble for about 2 ns with the time step of 1 fs. The production runs were then carried out under NVT ensemble for 20 ns. The trajectories were collected from the last 10 ns and the radial distribution functions (RDFs) were computed.

The water molecule interaction has been described by SPC/E model [10] in which the bond distances and angles of water molecule were kept constant [11]. The DREIDING

force-field [12] was used for interactions of other atom types. The Lennard-Jones (LJ) parameters for different types of atoms (σ_{ij}, ε_{ij}) are taken from pure types (σ_{ii}, ε_{jj}) following the Lorentz-Berthelot mixing rule [13], which is written as

$$\sigma_{ij} = \frac{\sigma_{ii} + \sigma_{jj}}{2}; \varepsilon_{ij} = \sqrt{\varepsilon_{ii}\varepsilon_{jj}} \quad (3)$$

All partial atomic charges except for water molecules, were extracted from the calculations by using the ORCA program. The HF/6-31G(d) theory and the electrostatic potential fitting (ESP) of CHELPG [14] have been used.

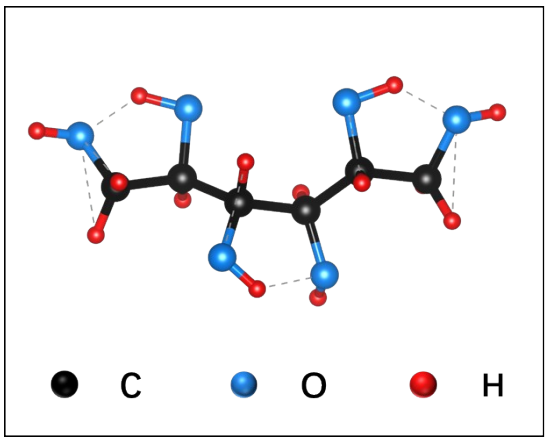

Figure S1 Structure of Mannitol.

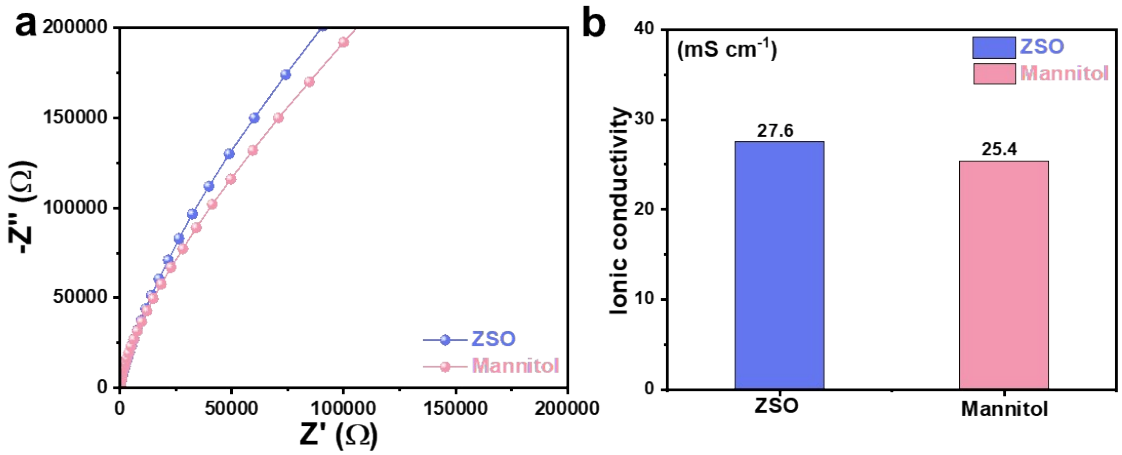

Figure S2 (a) Nyquist plots and (b) calculated ionic conductivity of $ZnSO_4$ and $ZnSO_4$+Mannitol electrolytes.

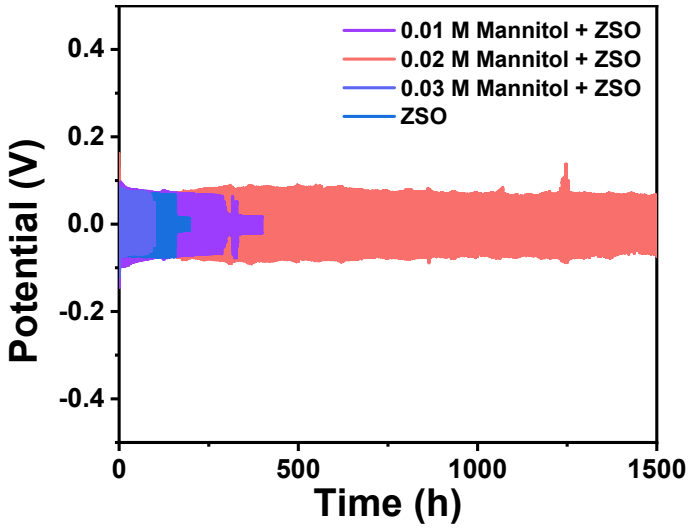

Figure S3 Cycling performance of Zn/Zn symmetrical batteries in 0.01 M Mannitol+ZSO, 0.02 M Mannitol+ZSO, 0.03 M Mannitol+ZSO, and ZSO electrolytes.

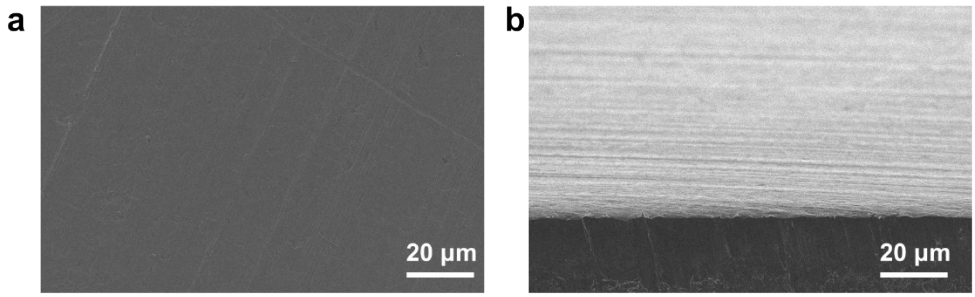

Figure S4 SEM images of pristine zinc metal anode.

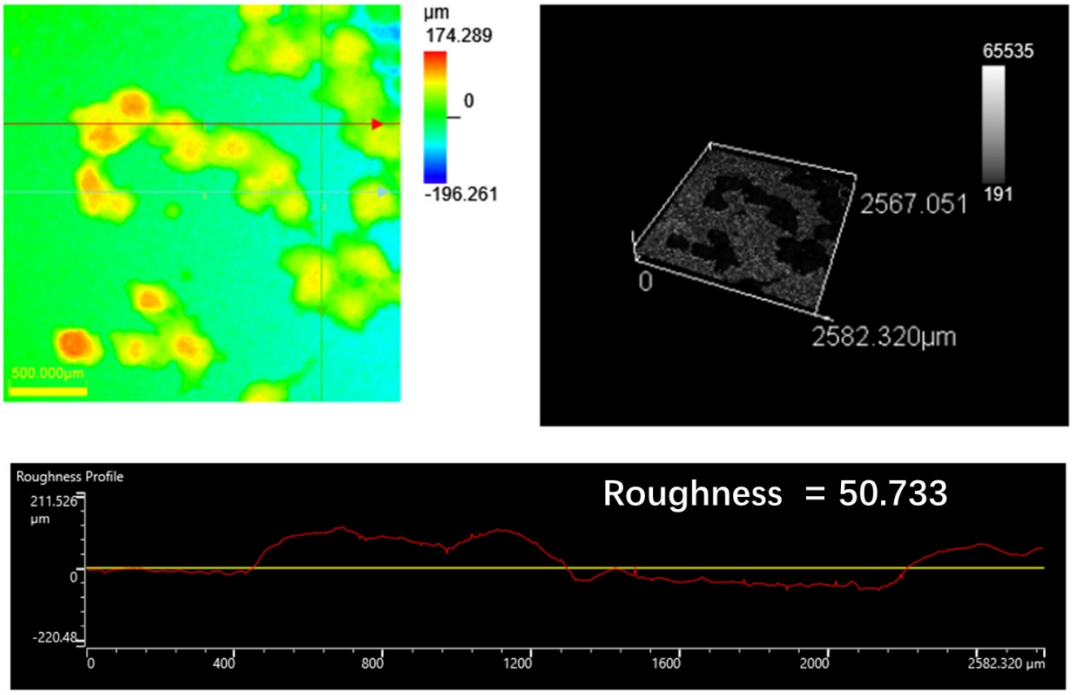

Figure S5 Roughness of Zn anode after 100 cycles in ZSO electrolyte.

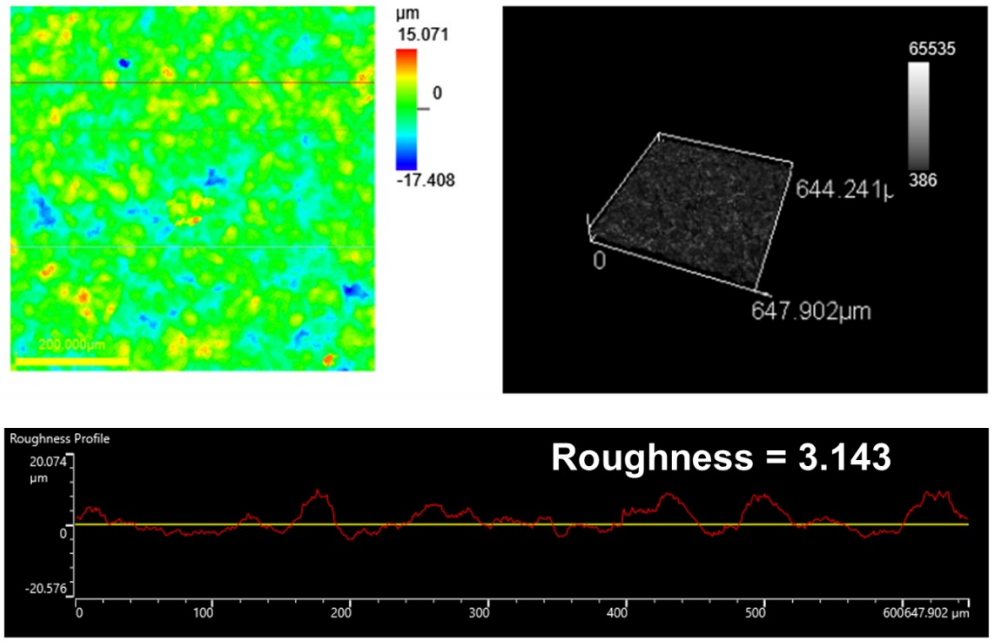

Figure S6 Roughness of Zn anode after 100 cycles in ZSO+Mannitol electrolyte.

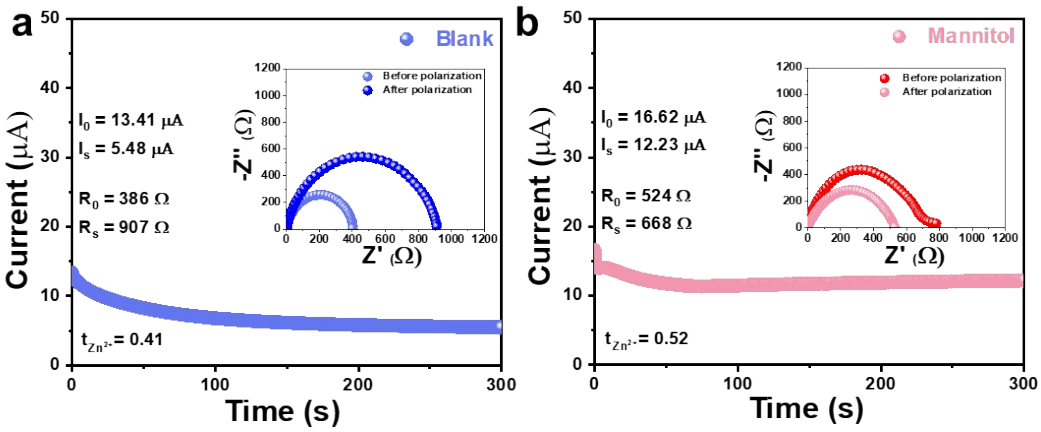

Figure S7 Measurements of Zn^{2+} transference number. Current-time plots of Zn symmetric cells with (a) $ZnSO_4$ and (b) $ZnSO_4$+Mannitol after polarization at 10 mV for 300 s. The insets are the impedance spectra before and after polarization. The transference number of Zn^{2+} (t_{Zn2+}) was evaluated by the following equation [15]:

$$t_{Zn^{2+}} = \frac{I_s(\Delta V - I_0 R_0)}{I_0(\Delta V - I_s I_s)}$$

where ΔV is the constant polarization voltage applied (10 mV here), I_0 and R_0 are the initial current and resistance, and I_s and R_s are the steady-state current and resistance, respectively.

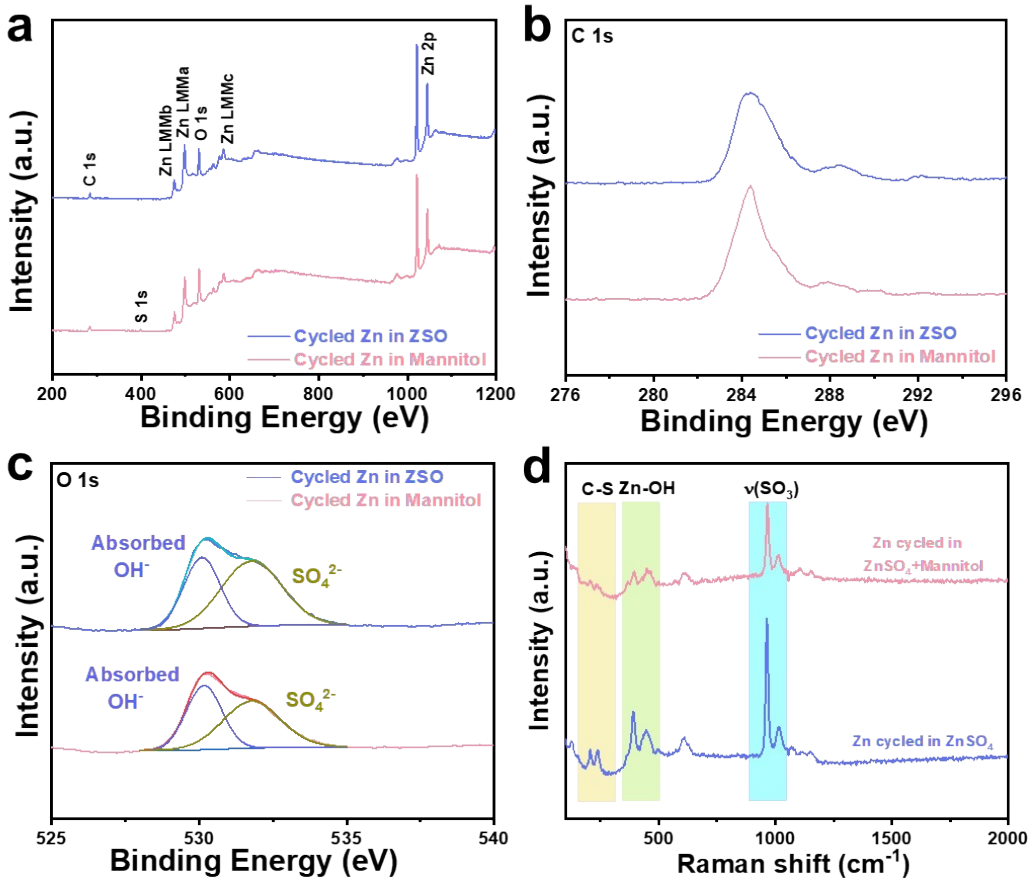

Figure S8 (a) XPS survey, (b) C 1s, (c) O 1s, and (d) Raman spectra of cycled Zn anode in $ZnSO_4$ and $ZnSO_4$+Mannitol.

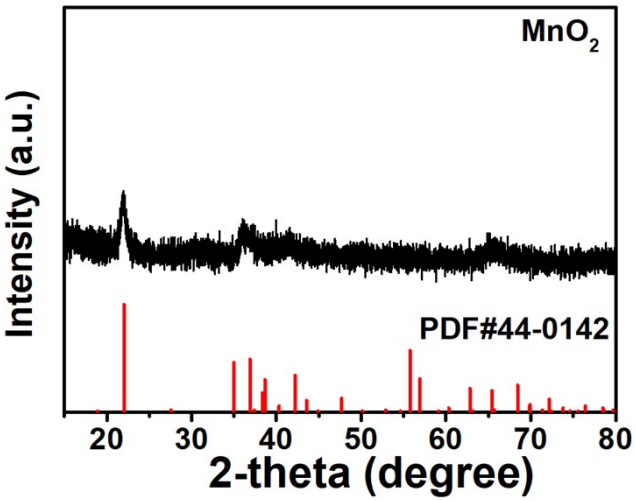

Figure S9 XRD pattern of MnO_2.

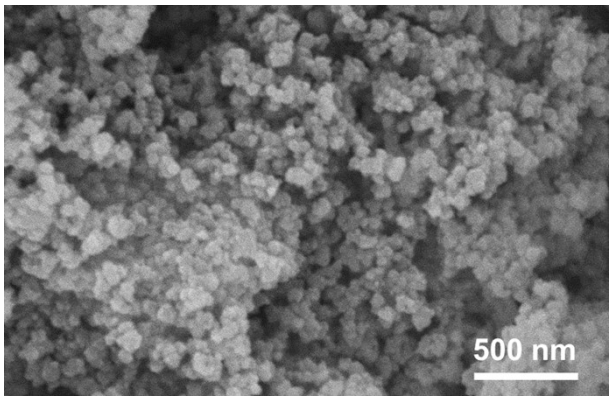

Figure S10 SEM image of MnO_2.

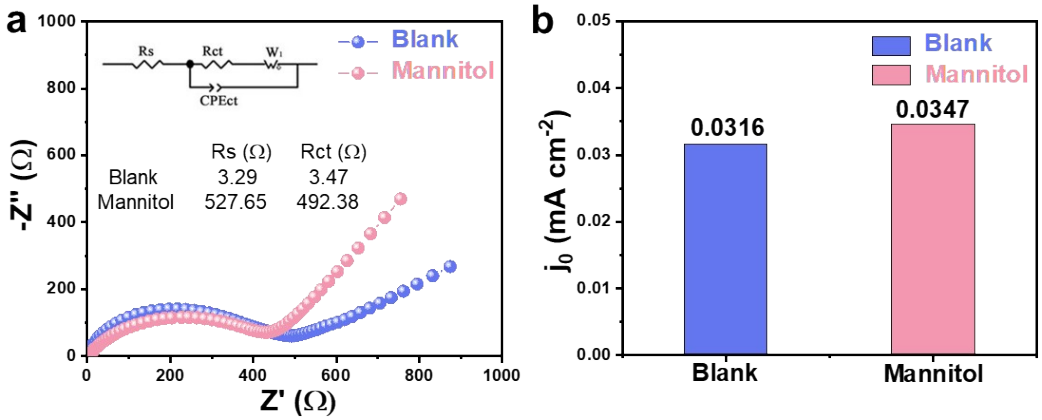

Figure S11 (a) Nyquist plots and equivalent circuits. (b) Comparison of the exchange current density (j_0) of MnO_2 electrodes in ZSO and Mannitol electrolytes.

Table S1 Performance comparison of Zn/Zn symmetric battery of this work and other reported works.

Strategies	Lifespan (h)	Ref
Methanol	400 (1 mA cm^{-2}; 0.5 mAh cm^{-2})	16
Ethanol	190 (1 mA cm^{-2}; 1 mAh cm^{-2})	17
Ethylene glycol	150 (2 mA cm^{-2}; 1 mAh cm^{-2})	18
Propylene glycol	1100 (1 mA cm^{-2}; 1 mAh cm^{-2})	19
Polyvinyl alcohol	300 (5 mA cm^{-2}; 5 mAh cm^{-2})	20
1,2,5,6-hexanetetraol	1400 (1 mA cm^{-2}; 1 mAh cm^{-2})	21
MOF-PVDF/Zn	500 (1 mA cm^{-2}; 0.5 mAh cm^{-2})	22
Lignin@Nafion/Zn	376 (0.2 mA cm^{-2}, 0.2 mA cm^{-2})	23
100TiO_2@Zn	150 (1 mA cm^{-2}; 0.5 mAh cm^{-2})	24
Zn@C	200 (1 mA cm^{-2}; 1 mAh cm^{-2})	25
Nano-$CaCO_3$/Zn	836 (0.25mA cm^{-2}; 0.05 mAh cm^{-2})	26
CNT/Zn	200 (2 mA cm^{-2}; 22 mAh cm^{-2})	27
$NaTi_2(PO_4)_3$	240 (1 mA cm^{-2}; 1 mAh cm^{-2})	28
Al_2O_3@Zn	500 (1 mA cm^{-2}; 1 mAh cm^{-2})	29
PiZn	300 (4 mA cm^{-2}; 2 mAh cm^{-2})	30
LM/Zn	500 (1 mA cm^{-2}; 0.5 mAh cm^{-2})	31
Sodium lignosulfonate additive	600 (0.5 mA cm^{-2}; 0.5 mAh cm^{-2})	32
Arginine additive	500 (0.5 mA cm^{-2}; 0.5 mAh cm^{-2})	33
Urea additive	700 (1 mA cm^{-2}; 1 mAh cm^{-2})	34
TBA_2SO_4 additive	300 (2 mA cm^{-2}; 2 mAh cm^{-2})	35
Mannitol additive	**1500 (1 mA cm^{-2}; 1 mAh cm^{-2})**	**This work**
	600 (4 mA cm^{-2}; 4 mAh cm^{-2})	**This work**

Table S2 DOD comparison of Zn/Zn symmetric battery of this work and other reported works.

Additive	Current density (mA cm^{-2}) /Capacity (mAh cm^{-2})	DOD	Time (h)	Ref.
Sorbitol	2.5/12.5	30%	175	[36]
Xylitol	5/10	56.9%	180	[37]
Sulfonamide	20/20	34.5%	100	[38]
Rb_2SO_4	5/5	42.78%	60	[39]
Chlorophyll	10/10	17.3%	45	[40]
Tetramethylurea	20/20	34.5%	100	[41]
D-trehalose dihydrate	1/1	1.7%	200	[42]
$CeCl_3$	40/10	17.3%	170	[43]
Mannitol	**2.5/12.5**	**55%**	**175**	**This work**

References

1. Z. Qu, M. Zhu, Y. Yin, Y. Huang, H. Tang, J. Ge, Y. Li, D. D. Karnaushenko, D. Karnaushenko and O. G. Schmidt, *Adv. Energy Mater.*, 2022, **12**, 2200714.
2. F. B. Van Duijneveldt, J. G. van Duijneveldt-van de Rijdt and J. H. van Lenthe, *Chem. Rev.*, 1994, **94**, 1873-1885.
3. B. Paizs and S. Suhai, *J. Comput. Chem.*, 1998, **19**, 575-584.
4. R. Chanajaree, M. Sriuttha, V. S. Lee and K. Wittayanarakul, *J. Mol. Liq.*, 2021, **322**, 114507.
5. F. Neese, *Wiley Interdisciplinary Reviews: Computational Molecular Science*, 2012, **2**, 73-78.
6. I. T. Todorov, W. Smith, K. Trachenko and M. T. Dove, *J. Mater. Chem.*, 2006, **16**,

1911-1918.

7. S. Nosé, *Mol. Phys.*, 1984, **52**, 255-268.

8. W. G. Hoover, *Phys. Rev. A*, 1985, **31**, 1695.

9. P. P. Ewald, *Ann. Phys.*, 1921, **369**, 253-287.

10. H. Berendsen, J. Grigera and T. Straatsma, *J. Phys. Chem.*, 1987, **91**, 6269-6271.

11. M. P. Allen and D. J. Tildesley, *Computer simulation of liquids*, Oxford university press, 2017.

12. S. L. Mayo, B. D. Olafson and W. A. Goddard, *J. Phys. Chem.*, 1990, **94**, 8897-8909.

13. H. A. Lorentz, *Ann. Phys.*, 1881, **248**, 127-136.

14. C. M. Breneman and K. B. Wiberg, *J. Comput. Chem.*, 1990, **11**, 361-373.

15. X. Zeng, J. Mao, J. Hao, J. Liu, S. Liu, Z. Wang, Y. Wang, S. Zhang, T. Zheng, J. Liu, P. Rao and Z. Guo, *Adv. Mater.*, 2021, **33**, 2007416.

16. J. Hao, L. Yuan, C. Ye, D. Chao, K. Davey, Z. Guo and S.-Z. Qiao, *Angew. Chem. Int. Ed.*, 2021, **60**, 7366-7375.

17. P. Hu, X. Luo, T. Hu, S. Chen, D. Li, Y. Chen and F. Li, *ACS Appl. Mater. Interfaces*, 2023, **15**, 5180-5190.

18. N. Chang, T. Li, R. Li, S. Wang, Y. Yin, H. Zhang and X. Li, *Energy Environ. Sci.*, 2020, **13**, 3527-3535.

19. Y. Shang, P. Kumar, T. Musso, U. Mittal, Q. Du, X. Liang and D. Kundu, *Adv. Funct. Mater.*, 2022, **32**, 2200606.

20. X. Chen, W. Li, S. Hu, N. G. Akhmedov, D. Reed, X. Li and X. Liu, *Nano Energy*, 2022, **98**, 107269.

21. Q. Hu, J. Hu, L. Li, Q. Ran, Y. Ji, X. Liu, J. Zhao and B. Xu, *Energy Storage Mater.*, 2023, **54**, 374-381.

22. M. Liu, L. Yang, H. Liu, A. Amine, Q. Zhao, Y. Song, J. Yang, K. Wang and F. Pan, *ACS Appl. Mater. Interfaces*, 2019, **11**, 32046-32051.

23. D. Yuan, W. Manalastas Jr, L. Zhang, J. J. Chan, S. Meng, Y. Chen and M. Srinivasan, *ChemSusChem*, 2019, **12**, 4889-4900.

24. K. Zhao, C. Wang, Y. Yu, M. Yan, Q. Wei, P. He, Y. Dong, Z. Zhang, X. Wang and L. Mai, *Adv. Mater. Interfaces*, 2018, **5**, 1800848.

25. W. Li, K. Wang, M. Zhou, H. Zhan, S. Cheng and K. Jiang, *ACS Appl. Mater. Interfaces*, 2018, **10**, 22059-22066.

26. L. Kang, M. Cui, F. Jiang, Y. Gao, H. Luo, J. Liu, W. Liang and C. Zhi, *Adv. Energy Mater.*, 2018, **8**, 1801090.

27. Y. Zeng, X. Zhang, R. Qin, X. Liu, P. Fang, D. Zheng, Y. Tong and X. Lu, *Adv. Mater.*, 2019, **31**, 1903675.

28. M. Liu, J. Cai, H. Ao, Z. Hou, Y. Zhu and Y. Qian, *Adv. Funct. Mater.*, 2020, **30**, 2004885.

29. H. He, H. Tong, X. Song, X. Song and J. Liu, *J. Mater. Chem. A*, 2020, **8**, 7836-7846.

30. M. Zhu, J. Hu, Q. Lu, H. Dong, D. D. Karnaushenko, C. Becker, D. Karnaushenko, Y. Li, H. Tang and Z. Qu, *Adv. Mater.*, 2021, **33**, 2007497.

31. D. Han, S. Wu, S. Zhang, Y. Deng, C. Cui, L. Zhang, Y. Long, H. Li, Y. Tao and Z. Weng, *Small*, 2020, **16**, 2001736.

32. W. Zhou, M. Chen, Q. Tian, J. Chen, X. Xu, X. Han and J. Xu, *J. Colloid. Interf. Sci.*, 2021, **601**, 486-494.

33. Z. Chen, H. Chen, Y. Che, L. Cheng, H. Zhang, J. Chen, F. Xie, N. Wang, Y. Jin and H. Meng, *ACS Sustain. Chem. Eng.*, 2021, **9**, 6855-6863.

34. Z. Hou, M. Dong, Y. Xiong, X. Zhang, H. Ao, M. Liu, Y. Zhu and Y. Qian, *Small*, 2020, **16**, 2001228.

35. A. Bayaguud, X. Luo, Y. Fu and C. Zhu, *ACS Energy Lett.*, 2020, **5**, 3012-3020.

36. M. Qiu, P. Sun, A. Qin, G. Cui and W. Mai, *Energy Storage Mater.*, 2022, **49**, 463-470.

37. H. Wang, W. Ye, B. Yin, K. Wang, M. S. Riaz, B.-B. Xie, Y. Zhong and Y. Hu, *Angew. Chem. Int. Ed.*, 2023, **62**, e202218872.

38. C. Huang, F. Huang, X. Zhao, Y. Hao, Y. Yang, Y. Qian, G. Chang, Y. Zhang, Q. Tang, A. Hu and X. Chen, *Adv. Funct. Mater* 2023, **33**, 2210197.

39. X. Zhang, J. Chen, H. Cao, X. Huang, Y. Liu, Y. Chen, Y. Huo, D. Lin, Q. Zheng and K.-h. Lam, *Small*, 2023, **n/a**, 2303906.

40. Y.-T. Xu, M.-J. Gong, Y. Zheng, H. Xu, A. Li, S.-i. Sasaki, H. Tamiaki, X.-X. Zeng, X.-W. Wu and X.-F. Wang, *Nano Letters*, 2023, **23**, 5722-5730.

41. Z. Li, Y. Liao, Y. Wang, J. Cong, H. Ji, Z. Huang and Y. Huang, *Energy Storage Mater.*, 2023, **56**, 174-182.

42. H. Peng, X. Wang, F. Yang, Z. Liu, H. Lei, S. Cui, X. Xie and G. Ma, *Chem. Eng. J.*, 2023, **474**, 145864.

43. Z. Hu, F. Zhang, Y. Zhao, H. Wang, Y. Huang, F. Wu, R. Chen and L. Li, *Adv. Mater.*, 2022, **34**, 2203104.